Thermocapillary migration of long bubbles in polygonal tubes. II. Experiments

E. Lajeunesse
Institut de Physique de Globe de Paris, 4 place Jussieu, 75252 Paris cedex 05, France

G. M. Homsy
Department of Mechanical and Environmental Engineering, University of California–Santa Barbara, Santa Barbara, California 93106-5070

(Received 16 July 2002; accepted 24 October 2002; published 6 January 2003)

We study experimentally the thermocapillary migration of a long gas bubble in a horizontal pipe of rectangular cross section. An imposed axial temperature gradient produces a gradient of surface tension leading to a steady migration of the bubble towards the hotter region. The bubble velocity is found to be independent of bubble length for sufficiently long bubbles, and to vary linearly with the temperature gradient. For pipes of small vertical dimension, gravity is negligible and the measurements of the bubble velocity are in good agreement with the zero gravity theory of Mazouchi and Homsy [Phys. Fluids **13**, 1594 (2001)]. In larger pipes, gravity is no longer negligible and the bubble is observed to move faster than that theory predicts. A simple calculation taking into account the combined effect of buoyant rise and thermocapillary stress accounts for these results.
 [DOI: 10.1063/1.1531617]

I. INTRODUCTION

This is the third in a series of papers[1,2] regarding thermocapillary migration of bubbles in microchannels, motivation for which has been given in Ref. 1. The essential feature of such problems is that the surface tension gradient resulting from an imposed temperature gradient causes interfacial flow from regions of low tension to region of higher tension. For most liquids, this implies a flow towards the colder region. As a result of mass conservation, the bubble then migrates towards the hotter region.

Parallel flow solutions[3,4] did not allow the determination of the bubble migration velocity, as they do not determine the thickness of the liquid film between the bubble and the wall. Wilson[5] and Mazouchi and Homsy[1] analyzed the thermocapillary migration of a long bubble in a *circular* pipe by means of a Bretherton-type[7] matched expansion. Assuming a temperature distribution determined by conduction (small Peclet number) and negligible gravity effects on the bubble shape (small Bond number), Mazouchi and Homsy[1] calculated the migration velocity in the small capillary number limit and found that the bubble velocity varies as the fifth power of the temperature gradient.

However, as discussed by Wong *et al.*,[8,9] a circular capillary lacks corners that characterize the geometry of many practical situations, e.g., the pores in a porous media or microchannels in MEMS devices. For this reason, Mazouchi and Homsy[2] also considered the thermocapillary migration of long bubbles in polygonal tubes in the small Bond number limit. They found that most of the liquid bypasses the bubble through the corners of the tube where a continuous liquid is present. This has two consequences for our problem. First, since the thermocapillary flow is, to a first approximation, a parallel flow in the corner regions, the bubble velocity varies linearly with the temperature gradient to leading order,[2] i.e.,

$$U_b = \lambda_0 \frac{\gamma_T a}{\mu} \beta, \tag{1.1}$$

where $\gamma_T = -\partial\sigma/\partial T$ is the temperature coefficient of surface tension, a is a characteristic dimension and μ is the liquid viscosity. λ_0 is a function of the aspect ratio B of the pipe cross section and is tabulated in Ref. 2. Second this migration velocity is much larger than it would be in a cylindrical tube, which is the distinguishing feature between the two types of cross sections and makes the polygonal pipe more attractive in the context of the applications.

In this article, we report the results of an experimental investigation of the thermocapillary migration of long gas bubbles in horizontal pipes of rectangular cross section. Our objective is to measure the velocity of the bubble, U_b, in a well-controlled and well-characterized temperature gradient β. Since the pioneering work of Young *et al.*,[10] a large amount of experimental work has addressed the issue of the thermocapillary migration of bubbles or droplets in liquids of large extent. To our knowledge, the present study is the first to consider the case of bubble migration in confined geometries in a quantitative way. We emphasize that our objectives are broader than a simple verification of Eq. (1.1), whose derivation involves many assumptions. Our objectives are to measure the migration velocity over a wide range of parameters, characterizing the parametric dependence, and (of course) comparing with Eq. (1.1) where appropriate.

The paper is organized as follows. In Sec. II, we introduce the fluids used and the scalings in the problem. Section III is dedicated to the description of the experimental setup and procedure. The experimental results are presented in Sec.

TABLE I. Physical properties of the silicon oil used in the experiments, ρ, μ, α, σ, and κ are the density, viscosity, the thermal expansion coefficient, the surface tension and the thermal diffusivity, respectively. $\gamma_T = -\partial\sigma/\partial T$ is the temperature coefficient of surface tension.

Fluid	ρ (Kg.m^{-3})	μ (Pa.s^{-1})	α (K^{-1})	σ (N.m^{-1})	γ_T (N.m^{-1}.K^{-1})	κ (m^{2}s^{-1})
Dow Corning 200 (5 cs)	913	4.56×10^{-3}	1.05×10^{-3}	1.97×10^{-2}	7.2×10^{-5} [a]	8.99×10^{-8}
Dow Corning 200 (0.65 cs)	758	4.93×10^{-4}	1.34×10^{-3}	1.59×10^{-2}	8.0×10^{-5}	7.7×10^{-8}

[a]Value interpolated from data for other viscosities.

IV and discussed in Sec. V. The paper ends with a summary of the results and conclusions.

II. FLUID PROPERTIES AND SCALINGS

The experiments were performed using two Dow Corning 200 silicon oils of differing viscosities (0.65 cs and 5 cs), chosen for their low susceptibility to surface contamination. Their properties are tabulated in Table I. As documented below, we worked with pipes whose characteristic dimension was on the order of a few millimeters.

Our typical range of parameters relate to the theory of Mazouchi and Homsy[2] in the following way. These authors neglected gravity and assumed small Reynolds (*Re*), Péclet (*Pe*), and capillary (*Ca*) numbers. As documented below, our experiments involved small *Re* ranging from 10^{-4} to 10^{-1}, small *Pe* ranging from 10^{-3} to 1 and small *Ca* ranging from 10^{-8} to 10^{-6}. Gravity was negligible in some but not all of our experiments, which impacts them in two different ways. First, the density difference between the gas and the surrounding liquid causes the bubble to be asymmetrically placed in the cross section of the pipe. This buoyant rise of the static bubble is characterized by the Bond number

$$Bo = \frac{\rho g a^2}{\sigma}, \tag{2.1}$$

where ρ is the density of the liquid, g is the gravity, σ is the surface tension between the gas and the liquid, and $t = 2a$ is the vertical height of the pipe. Mazouchi and Homsy[2] worked in the zero Bond number limit so that they only addressed a symmetrically placed bubble. Experimentally, we varied the height from $t = 0.3$ mm to $t = 3$ mm. As a result, *Bo* ranged from $Bo = 10^{-2}$, where buoyant rise is negligible, to $Bo = 1$, where the bubble can be expected to be asymmetrically placed.

The second effect of gravity comes from the existence of a horizontal temperature gradient in the liquid along the pipe. This leads to buoyant convection in the liquid which may affect the bubble migration by exerting additional forces on the bubble. As is well-known in other contexts[6] this effect is characterized by the ratio G of the buoyant forces to the thermocapillary forces (sometimes referred to as the dynamic Bond number)

$$G = \frac{\rho \alpha g a^2}{\gamma_T}, \tag{2.2}$$

where α is the coefficient of thermal expansion.

For small G, we expect the bubble to be unaffected by buoyant convection. G was never larger than $O(1)$ over the range of parameters studied. As such, natural convection played an insignificant role in our experiments, and the primary effect of gravity was buoyant rise of the static bubble.

III. APPARATUS AND PROCEDURE

A. Schematic of apparatus

The experiment is conceptually simple, i.e., to establish and characterize a steady axial temperature gradient, $\beta(x)$, introduce a bubble into a tube, and measure its migration velocity. We accomplish this by the apparatus shown in Fig. 1(a). A glass pipe of rectangular cross section is held between two reservoirs and passes through them and through flanges at both ends that facilitate assembly and disassembly. The two ends of the pipe are joined to flexible tubing (not shown), allowing the introduction of the bubble. Each reservoir is connected to a thermostatically controlled bath, allowing a constant applied temperature difference $\Delta T = T_h - T_c$ to be maintained within an accuracy of $\pm 0.5\,^{\circ}$C. The whole setup lies on a plate fitted with leveling screws to ensure horizontality.

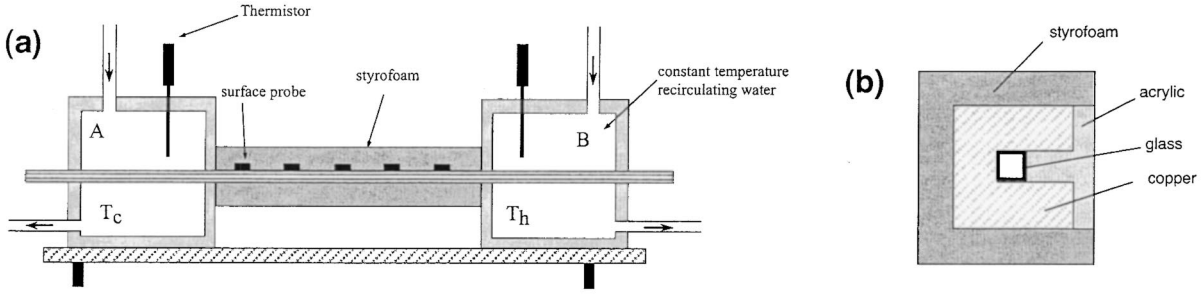

FIG. 1. Schematic of experimental apparatus. (a) Side view. (b) Cross section of the pipe.

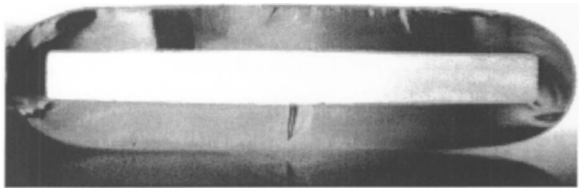

FIG. 2. The cross section of the 0.3×3 mm pipe.

The size and aspect ratio of the pipe were varied by using four different rectangular pipes (Whale Apparatus, Hellerton, Pennsylvania, model ST-8100, ST-102, ST-103, and RT-3530), the cross-sections of which were respectively equal to (height×width) 1×1 mm, 2×2 mm, 3×3 mm, and 0.3×3 mm. Photographs of the pipe cross sections taken with a camera connected to a microscope verified their dimensions and allowed examination of the shape of the corners. As can be seen in the example shown in Fig. 2, the corners are only slightly rounded.

B. Establishing the temperature gradient

The key issue to establish, control, and measure the temperature gradient. In order to do so, the glass pipe was surrounded on three sides by a copper U-channel as sketched in Fig. 1(b). The thickness of the copper walls was 2.5 mm. The U-channel was closed by an insulating acrylic wall and the entire assembly was in turn enclosed inside a thermally insulating styrofoam U-channel [Fig. 1(b)] of thickness 1 cm. Thermal contact between the copper and the glass pipe was maintained with a thin layer of silicone oil. The temperature $T(x)$ was measured within an accuracy of $\pm 0.1\,^{\circ}\mathrm{C}$ along the copper surface by mean of five surface thermistor probes placed between the copper and the styrofoam layer. Due to the small thickness of the pipe walls (from 0.1 to 0.5 mm), the surface temperature was assumed to be very close to the oil temperature inside the pipe. The time necessary to reach thermal equilibrium was on the order of one hour.

Figure 3(a) shows an example of a typical measured temperature distribution, the general shape of which is that expected from the so-called fin equations. Apart from the abrupt variation near the reservoirs, $T(x)$ is very nearly linear over most of the pipe: Therefore, the temperature gradient for any given experiment was evaluated by at least square fit of the experimental points in the region of interest, as indicated by the solid line in Fig. 3(a).

C. Experimental procedure

The experimental procedure was the following. The pipe was filled with a particular liquid. Once thermal equilibrium had been reached and a steady axial temperature profile established, a bubble of air was introduced by means of a syringe with a flexible needle into the region of the pipe surrounded by the colder reservoir A (see Fig. 1). The plate was then tilted slightly until the bubble left the reservoir A and entered the region of the pipe where the temperature varies. As a result, the bubble moved towards the hotter reservoir B and its position was recorded at regular time intervals using a CCD camera connected to a computer via a Scion LG3

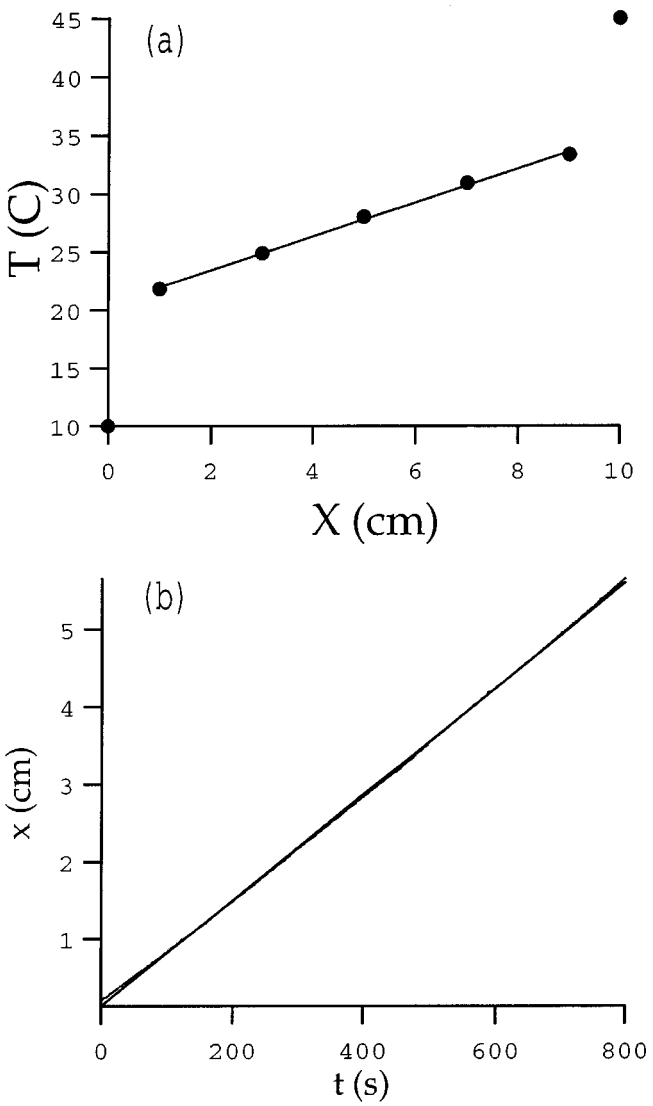

FIG. 3. Typical data for the 2×2 mm pipe filled with a V0.65 silicone oil. The temperature difference applied along the pipe is $\Delta T = 35$ K. (a) Temperature as a function of the position x (cm) along the pipe. The circles correspond to experimental temperature measurements and the solid line is a linear least-squares fit of the data. The value of the temperature gradient obtained under these conditions is $\beta = 1.45$ K/cm. (b) Position x (cm) of the rear cap of a bubble as a function of the time t (s) for the same experimental conditions.

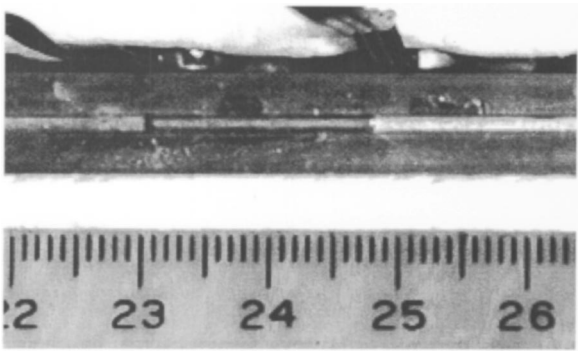

FIG. 4. An air bubble in a 1×1 mm pipe. The pipe is surrounded by copper walls and styrofoam. The thermal probes are also visible.

Framegrabber. Using the digitized images, an example of which is shown in Fig. 4, we measured the position of the bubble as a function of time.

Figure 3(b) shows a typical example of the displacement data obtained, which correspond to the temperature field displayed in Fig. 3(a). The bubble is seen to advance at a constant rate in the region of constant temperature gradient. The bubble velocity U_b was evaluated from a linear least-square fit of the experimental data in this linear region and measured as a function of the corresponding temperature gradient.

After the bubble reached the end of the pipe, it was brought back into the reservoir A by again tilting the plate. This enabled us to perform several experiments with the same bubble for various applied temperature differences. The horizontality of the pipe was tested by inverting the direction of the temperature gradient: The measured velocity was independent of the sign of the gradient, indicating that axial motion due to the tube not being horizontal was entirely negligible.

The possible influence of the age of the bubbles was investigated by performing experiments with bubbles of age ranging from a few minutes up to two weeks. We did not observe any significant dependence of the bubble velocity with its age, confirming the low susceptibility of silicon oil to surface contamination, especially in the closed system used here.

Finally, we investigated the effect of the size of the bubble by performing series of experiments keeping the same temperature gradient but varying the bubble length. We observed that the bubble migration velocity increases with the bubble length until it reaches $L_B \approx 10a$. For longer bubbles, the migration velocity does not depend on the bubble length. All our reported data are for these long bubbles.

IV. EXPERIMENTAL RESULTS

We performed several series of experiments working with a given pipe and a given oil and varying only the temperature gradient β. As a result, B and Bo were kept constant for each series of experiments.

Figure 5 displays the experimentally measured bubble velocity U_b as a function of β for a 0.3×0.3 mm pipe filled with the Dow Corning 200 V0.65 oil. In this case, $B=10$ and $Bo=1.05\times10^{-2}$. The migration velocity varies linearly with the temperature gradient and is in very good agreement with Eq. (1.1) which is shown by the solid line.

Figure 6 displays similar data but for a 2×2 mm pipe filled with the Dow Corning 200 V5 oil. In that case, $B=1$ and $Bo=4.5\times10^{-1}$. As in the previous case, the bubble velocity varies linearly with the temperature gradient, but with a speed that is slightly higher than the predictions of Mazouchi and Homsy.[2]

We conducted a large number of experiments, varying the temperature gradient, pipe size, and fluid. We performed experiments with two different aspect ratios $B=1$ and $B=10$. The bubble velocity was always observed to vary linearly with the temperature gradient for any given fixed values of B and Bo, but with a slope that depends on these parameters. Because of this linearity, it suffices to record the slope of the least-squares fits to data such as these in Figs. 5 and 6.

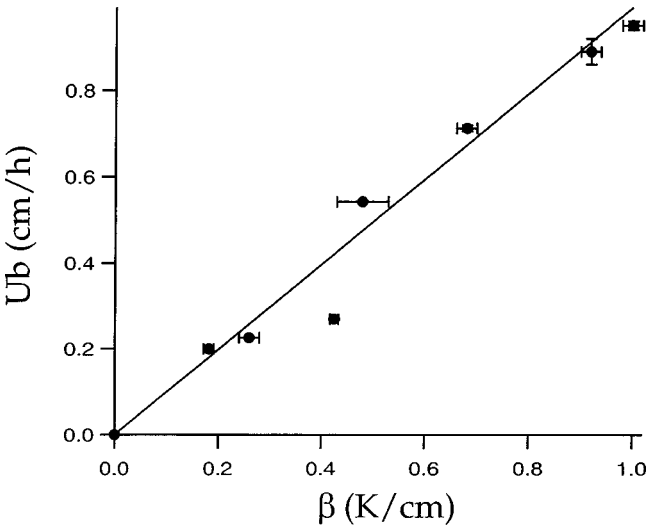

FIG. 5. Velocity of the bubble (cm/h) as a function of the temperature gradient (K/cm) for a 0.3×3 mm pipe and the Dow Corning 200 V0.65 oil. $B=10$ and $Bo=1.05\times10^{-2}$. The solid line is the theory of Mazouchi and Homsy (Ref. 2).

From each set of data, we deduced an experimental value λ_{ex} by scaling the measured slope by $\mu/\gamma_T a$. The complete set of results is tabulated in Table II, where we give the pipe size and aspect ratio, the liquid used, the value of λ_{ex}, together with the correlation coefficient, R, of the linear least-squares fit, the values of λ_0, and the Bond number Bo.

To be complete, we mention that for the Dow Corning 200 V0.65 oil in the 1×1 mm pipe, we observed a small deviation from the linearity in the limit of the large temperature gradients ($\beta>1$ K/cm). This effect might be due to non-negligible variation of the viscosity with the local tem-

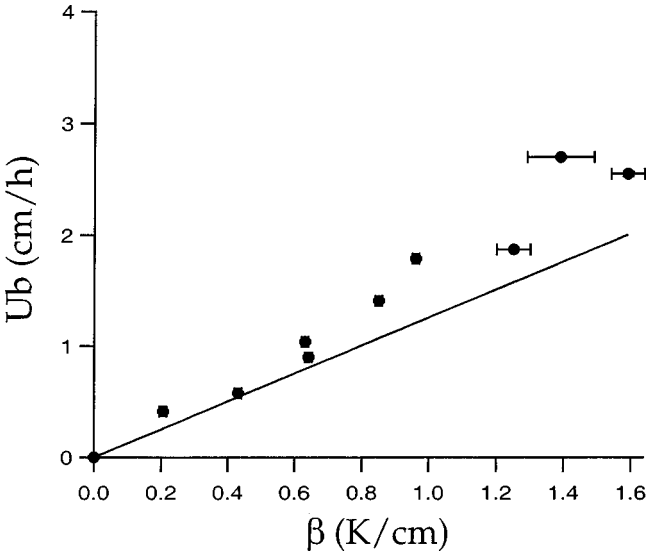

FIG. 6. Velocity of the bubble (cm/h) as a function of the temperature gradient (K/cm) for a 2×2 mm pipe and the Dow Corning 200 V5 oil. $B=1$ and $Bo=4.5\times10^{-1}$.

TABLE II. Experimental results.

Pipe	Oil	B	$>l_{exp}$	R	λ_0	B_0
0.3×3 mm	0.65 cst	10	1.1×10^{-3}	0.98	1.1×10^{-3}	1.05×10^{-2}
1×1 mm	0.65 cst	1	1.8×10^{-3}	0.99	2.2×10^{-3}	1.17×10^{-1}
1×1 mm	5 cst	1	2.4×10^{-3}	1	2.2×10^{-3}	1.14×10^{-1}
2×2 mm	0.65 cst	1	2.9×10^{-3}	0.98	2.2×10^{-3}	4.68×10^{-1}
2×2 mm	5 cst	1	3.0×10^{-3}	0.98	2.2×10^{-3}	4.55×10^{-1}
3×3 mm	0.65 cst	1	6.4×10^{-1}	0.98	2.2×10^{-3}	1.05
3×3 mm	5 cst	1	9.6×10^{-3}	0.96	2.2×10^{-3}	1.02
3×0.3 mm	0.65 cst	0.1	6.8×10^{-3}	0.99	1.1×10^{-4}	1.05

perature along the bubble. The compressibility of the bubble might also play a part: For this specific run, we observed the bubble length to increase up to 10% while migrating from the cold to the hot region. Alternatively, it may be due to the thin film corrections to Eq. (1). These data corresponding to large temperature gradients were not taken into account when calculating the value of λ_{ex}.

V. ANALYSIS AND DISCUSSION

A. Analysis of the experimental results

Table II, together with the implied linearity of U_b with β, are the main results of our work. At small values of *Bo* where gravity is negligible, λ_{ex} is close to λ_0. Therefore, in this regime where the assumptions of Mazouchi and Homsy[2] are fulfilled, theory and experiments are in very good agreement with *all aspects*. The migration velocity is observed to be independent of the bubble length, approximately proportional to the ratio $a\gamma_T/\mu$ and linear in the temperature gradient, with a coefficient that is accurately predicted by the zero gravity theory. This conclusion may be drawn for the two smallest pipe sizes. For the intermediate pipe size, 2×2 mm, the slope scales with $1/\mu$ as expected, but with a value of λ_{ex} slightly above the zero gravity theory. There are large positive deviations for the largest pipe studied.

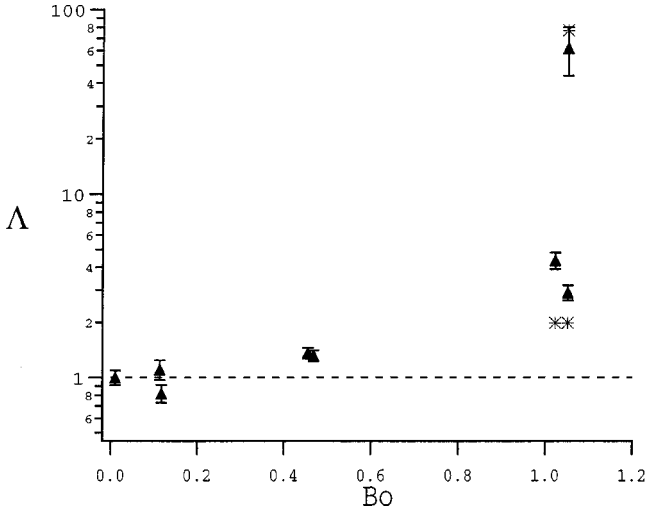

FIG. 7. The normalized slope as a function of the Bond number, *Bo*. Triangles: $\Lambda_{ex}=\lambda_{ex}\lambda_0$; Stars: The theoretical values, $\Lambda_{Bo}=\lambda_{Bo}/\lambda_0$, from the approximate theory of Sec. V.

We wish to assess the degree to which gravity plays a role in our experiments. In order to do so, we account for the effect of varying aspect ratio through the following procedure. The experimental values λ_{ex} were normalized by the corresponding theoretical value λ_0. The resulting number $\Lambda_{ex}=\lambda_{ex}/\lambda_0$ depends only on *Bo*: its departure from unity is a measure of the influence of gravity. It is plotted as a function of *Bo* in Fig. 7. As is evident from the figure, gravity is no longer negligible for $Bo=0(1)$. In this regime, Λ_{ex} is greater than one and generally increases with *Bo*, leading to migration velocities that can be two orders of magnitude above that of the zero gravity theory. In the next section, we give a simple theory that accounts for this Bond number dependence.

B. Effect of gravity on the bubble migration

The effect of buoyant rise is relatively straightforward to account for. Increasing *Bo* causes the bubble to be increasingly asymmetrically placed within the pipe. As a result, the thickness of the layer of liquid between the lower side of the bubble and the wall of the pipe increases to the point where a continuous film of liquid covers the bottom of the pipe. In the case of both the 3×3 mm and the 3×0.3 mm pipe, we clearly observed that the lower part of the bubble was not in contact with the pipe wall, as shown in Fig. 8. Consequently the bubble offers less resistance to the thermocapillary pumping of the liquid and both the flux of liquid and the bubble velocity are increased.

To calculate the effect of buoyant rise on the bubble speed, we considered a bubble asymmetrically placed within the pipe and calculated its velocity under the following simplified assumptions. We neglect the curvature of the bubble

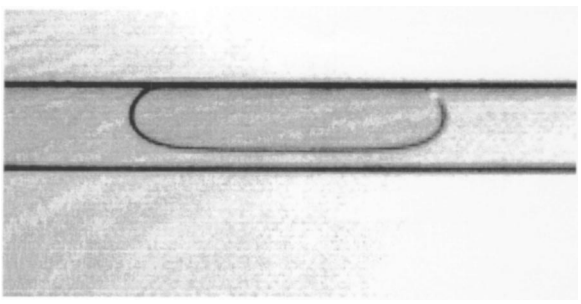

FIG. 8. The static shape of an air bubble in a 3×0.3 mm pipe filled with a Dow Corning 200 V0.65 oil. *Bo*=1.05. The thickness of the film of fluid below the bubble is 0.4 mm.

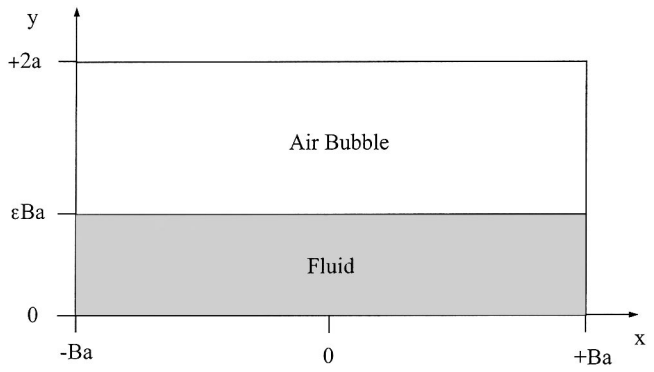

FIG. 9. Schematic of the cross section of a bubble asymmetrically placed within the pipe. The bubble is assumed to have a rectangular cross-section area.

in the cross-sectional plane and neglect the flux of liquid pumped through the top corner regions. As a result, the bubble is approximated as having a simple rectangular cross section as shown in Fig. 9. The height of the pipe is $t=2a$ and its aspect ratio is B; the thickness of the film of fluid below the bubble is taken to be ϵBa. With these assumptions, the flow is a parallel flow, and the equations describing the axial velocity u are

$$\frac{\partial^2 u}{\partial x^2}+\frac{\partial^2 u}{\partial y^2}=0, \tag{5.1}$$

$$u=0,\ x=\pm Ba,\quad y=0, \tag{5.2}$$

$$\frac{\partial u}{\partial y}=-\frac{\gamma_T \beta}{\mu},\quad y=\epsilon Ba. \tag{5.3}$$

Scaling x and y with respect to Ba and defining $W=\mu u/\gamma_T \beta Ba$, the preceding equation becomes

$$\frac{\partial^2 W}{\partial x^2}+\frac{\partial^2 W}{\partial y^2}=0, \tag{5.4}$$

$$W=0,\ x=\pm 1,\ y=0, \tag{5.5}$$

$$\frac{\partial W}{\partial y}=-1,\ y=\epsilon. \tag{5.6}$$

The set of equations (5.4)–(5.6) were solved using a finite difference method. From the solution, we express the thermocapillary flux through the bottom film as

$$Q=Q_0\frac{(Ba)^3 \gamma T \beta}{\mu}, \tag{5.7}$$

where Q_0 is the dimensionless flux computed by integrating $W(x,y)$ over the cross section of the liquid. Note that Q_0 only depends on the value of ϵ.

The bubble migration velocity is then deduced from the global mass balance as in Ref. 2

$$U_b S_b=Q, \tag{5.8}$$

where $S_b=a^2 B(4-2\epsilon B)$ is the bubble cross-sectional area. From Eqs. (5.7) and (5.8), we have

$$U_b=\frac{Q_0 B^2}{4-2\epsilon B}\frac{\gamma Ta\beta}{\mu}=\Lambda_{Bo}\frac{\gamma Ta\beta}{\mu}, \tag{5.9}$$

which, since it is based on parallel flow, is of the same form as Eq. (1.1). The coefficient $\lambda_{Bo}=Q_0 B^2/(4-2\epsilon B)$ depends both on the thickness of the film of fluid and on the pipe aspect ratio.

We measured the thickness of the film of fluid below the bubble from experimental photographs of the static bubble shapes, such as that in Fig. 8. For both fluids in the 3×3 mm pipe ($B=1$), the film thickness was measured to be 0.20 ± 0.02 mm so that $\epsilon=0.13$ and $\lambda_{Bo}=4.37\times 10^{-3}$. For the 3×0.3 mm pipe ($B=0.1$), the film thickness is 0.40 ± 0.02 mm, so that $\epsilon=2.7$ and $\lambda_{Bo}=8.46\times 10^{-3}$. In order to be compared with the experimental measurements reported in Fig. 7, the values of λ_{Bo} were normalized by the zero gravity theoretical value λ_0 calculated by Mazouchi and Homsy[2] for the same pipe aspect ratio. The results correspond to the stars in Fig. 7. As can be seen, they agree well with the experimental measurements. As a result, the additional thermocapillary flux pumped through the continuous film caused by buoyant rise seems to account for the increase of the bubble velocity when gravity effects are no longer negligible.

VI. SUMMARY

In summary, we have reported an experimental study of the thermocapillary migration of a long gas bubble in a horizontal pipe of rectangular cross section. An imposed axial temperature gradient produces a gradient of surface tension leading to a steady migration of the bubble towards the hotter region. We measured this migration velocity as a function of the temperature gradient for two different viscosity fluids, and for pipes of different size and aspect ratio. The bubble velocity is observed to vary linearly with the temperature gradient for any given fixed value of B and Bo (i.e., for a given pipe and a given oil), but with a slope that depends on these parameters.

For pipes of small thickness, gravity is negligible (small Bond number) and the measurements of the bubble velocity are in good agreement with the zero gravity theory of Mazouchi and Homsy.[2] In larger pipes, gravity is no longer negligible, the bubble is more and more asymmetrically placed within the pipe, and the results deviate from the simple theory. The thickness of the layer of liquid between the lower side of the bubble and the wall of the pipe increases so that the flux of liquid and the bubble velocity are increased. A simple theory accounts for these effects.

ACKNOWLEDGMENTS

This work was performed in the Department of Chemical Engineering, Stanford University. It was supported by the Chemical Sciences Division, Office of Basic Energy Services, U.S. Department of Energy.

[1] A. Mazouchi and M. Homsy, "Thermocapillary migration of long bubbles in cylindrical capillary tubes," Phys. Fluids **12**, 542 (2000).
[2] A. Mazouchi and G. M. Homsy, "Thermocapillary migration of long bubbles in polygonal tubes. I. Theory," Phys. Fluids **13**, 1594 (2001).

[3]M. M. Hasan and R. Balasubramaniam, ''Thermocapillary migration of a large gas slug in a tube,'' J. Thermophys. Heat Transfer **3**, 87 (1989).
[4]S. K. Wilson, ''The steady thermocapillary-driven motion of a large droplet in a closed tube,'' Phys. Fluids A **5**, 2064 (1993).
[5]S. K. Wilson, ''The effect of an axial temperature gradient on the steady motion of a large droplet in a tube,'' J. Eng. Math. **29**, 205 (1995).
[6]S. Ostrach, ''Low gravity flows,'' Annu. Rev. Fluid Mech. **14**, 313 (1982).
[7]F. P. Bretherton, ''The motion of long bubbles in tubes,'' J. Fluid Mech. **10**, 166 (1961).
[8]H. Wong, C. J. Radke, and S. Morris, ''The motion of long bubbles in polygonal capillaries. Part 1. Thin films,'' J. Fluid Mech. **292**, 71 (1995).
[9]H. Wong, C. J. Radke, and S. Morris, ''The motion of long bubbles in polygonal capillaries. Part 2. Drag, fluid pressure and fluid flow,'' J. Fluid Mech. **292**, 95 (1995).
[10]N. O. Young, J. S. Goldstein, and M. J. Block, ''The motion of bubbles in a vertical temperature gradient,'' J. Fluid Mech. **6**, 350 (1959).